

## Supporting Information

# Two Dimensional Silicon Nanowalls for Lithium Ion Batteries

Jiayu Wan,<sup>1,(a)</sup> Alex F. Kaplan,<sup>2,(a)</sup> Jia Zheng,<sup>3,(a)</sup> Xiaogang Han,<sup>1</sup> Yuchen Chen,<sup>1</sup> Nicholas J. Weadock,<sup>1</sup> Nicholas Faenza,<sup>1</sup> Teng Li,<sup>3,\*</sup> Jay Guo,<sup>2,\*</sup> and Liangbing Hu,<sup>1,\*</sup>

<sup>1</sup>*Department of Materials Science and Engineering, University of Maryland, College Park, MD, USA, 20742*

*\*Email: Binghu@umd.edu*

<sup>2</sup>*Department of Electrical Engineering and Computer Science, University of Michigan, Ann Arbor, MI, USA, 48109*

*\*Email: Guo@umich.edu*

<sup>3</sup>*Department of Mechanical Engineering, University of Maryland, College Park, MD, USA, 20742*

*\*Email: LiT@umd.edu*

*(a) These authors contribute equally to this work*

## 1. Modeling details

To gain insights on the nano-pore formation and stress generation during lithiation and delithiation, we have simulated the concurrent diffusion and mechanical deformation during initial lithiation and following delithiation of the amorphous silicon nanowall using finite

element package ABAQUS 6.10. The diffusion and elastic-perfectly plastic model is employed and the material undergoes elastic and/or plastic deformation where the von Mises yield criterion determines plastic yielding. The plastic deformation is governed by the J2-flow rule. The normalized lithium concentration and stress-strain fields are numerically solved by a fully-coupled implicit temperature-displacement procedure in ABAQUS/Standard, given that governing equations of diffusion is essentially equivalent to those of heat. During simulation the normalized lithium concentration and associated stress-strain deformation are updated incrementally. The normalized lithium concentration is defined as the current concentration (i.e.  $x$  in  $Li_xSi$ ) divided by the concentration at fully-lithiated stage ( $x = 4.2$ ) and it is equivalent to the “temperature” in above-mentioned numerical procedure. The lithiation-induced volumetric strain is equivalently to the “thermal strain” caused by “temperature” change. The coefficient of thermal expansion is chosen to be 0.6 and thus the accordingly volumetric expansion is 400% when the “temperature” in simulation (i.e. normalized lithium concentration) reaches 1.

The dimension of the nanowall is 600nm×900nm×50nm. Taking advantage of symmetry, only  $\frac{1}{4}$  of the nanowall is simulated in order to reduce the numerical expense, with symmetry boundary condition is employed at mid-planes  $z = 0$  and  $x = 0$ . The Young’s modulus and Poisson’s ratio of lithiated silicon are both assumed to vary linearly with Li concentration from 160 to 40 GPa and from 0.24 to 0.22 respectively <sup>[1,2]</sup>. The yielding stress of lithiated silicon is chosen to be 2GPa. Diffusivity of lithium in silicon is assumed to be a constant of  $10^{-13}$  cm<sup>2</sup>/s <sup>[3]</sup>. The amorphous silicon nano-wall is initially pristine and subjected to a constant C/5 charging/discharging rate at the outer surface. In the simulation, the lithiation half cycle is terminated when  $x_{average}$  reaches 2 and delithiation half cycle begins with the final lithium concentration and stress-strain field at the end of lithiation half cycle. The displacements at the

bottom surface of nanowall are all fixed to zero and all other outer surfaces are traction free.

## 2. Additional simulation results

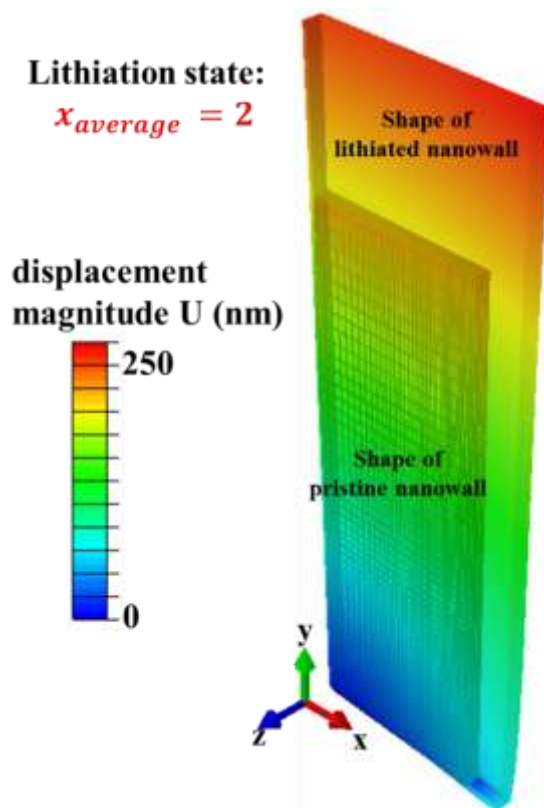


**Figure S1** Volume expansion before (pristine nanowall) and after lithiation half cycle ( $x_{average} = 2$ ).  $x_{average}$  reaches 2 at the end of the lithiation cycle, resulting in a ~200% volume expansion of the nanowall. Mesh of the pristine nanowall is also shown (Note: the triad is only used to show the directions of coordinate but it does NOT represent the real coordinate system of which the origin is at the center of the bottom surface. Same for **Figure S2**, **S3** and **S4**).

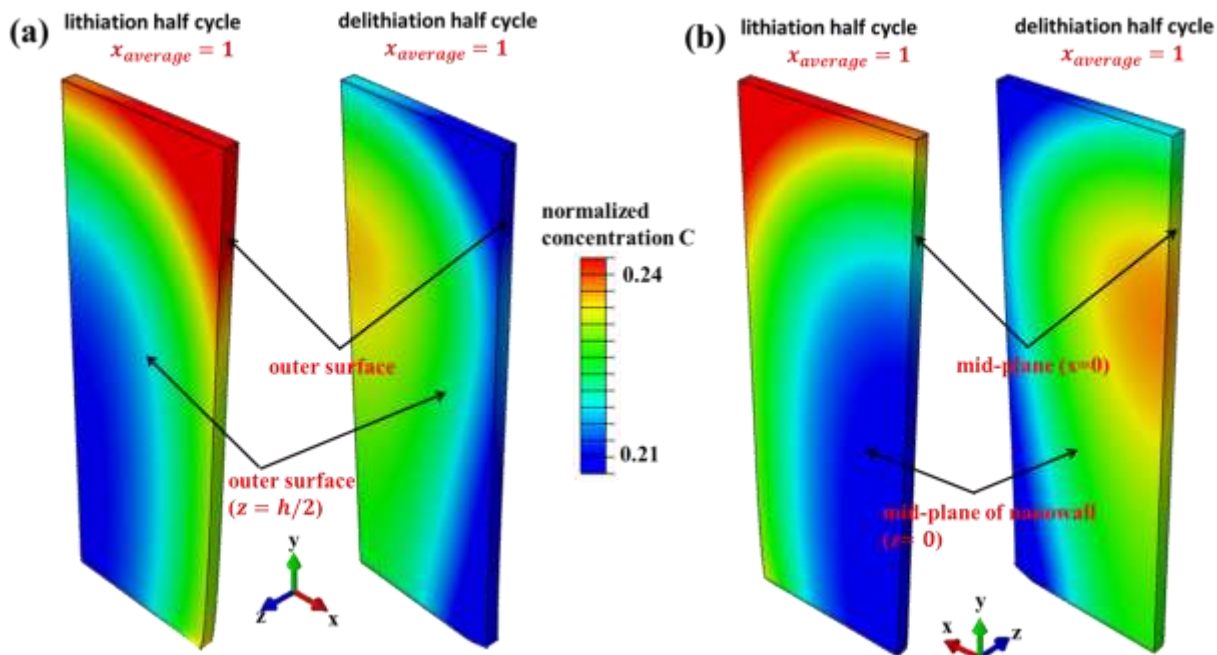


**Figure S2.** (a). Normalized Li concentration distribution at the outer surface during lithiation half cycle (left) and delithiation half cycle (right) when  $x_{average} = 1$ , from a perspective view. Concentration profile at the outer surface on the side of nanowall is also available from this perspective. Rotating the perspective view in (a) by  $180^\circ$  with respect to  $y$  axis gives (b) the perspective view of the similar plots at mid-planes ( $x = 0$  and  $z = 0$ ). During lithiation, concentration is higher near the outer surface but lower in the interior of nanowall; during delithiation, concentration is higher in the interior of nanowall but lower near the outer surface.

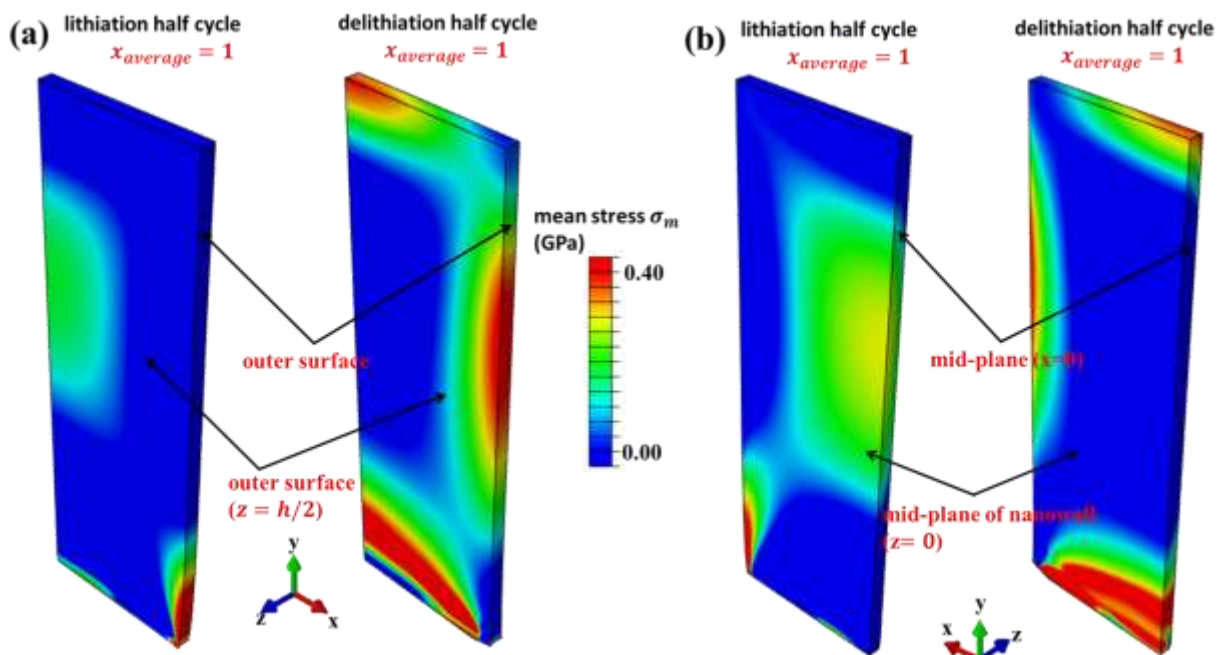


**Figure S3.** (a) Distribution of mean stress  $\sigma_m$  at the outer surface of the nanowall during lithiation half cycle (left) and delithiation half cycle (right) when  $x_{average} = 1$  from a perspective view. (b). The perspective view of the similar plots at the mid-planes ( $x = 0$  and  $z = 0$ ).

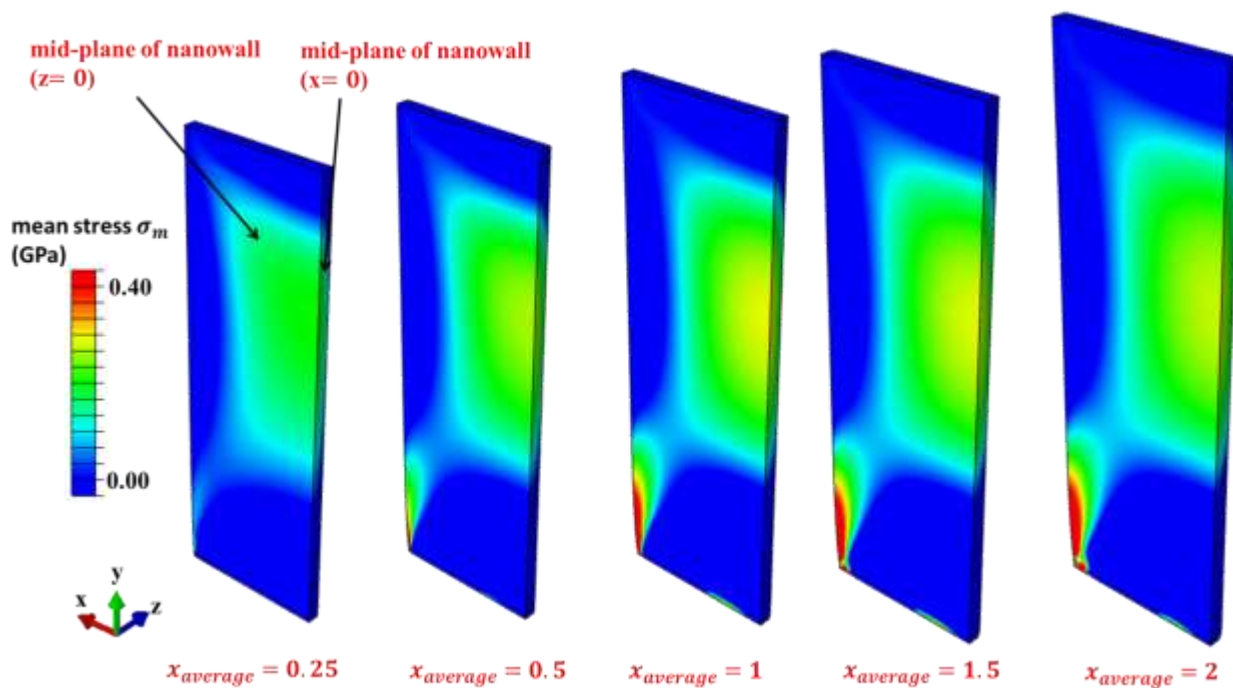


**Figure S4.** Mean stress  $\sigma_m$  evolution during lithiation half cycle. Note that the mean stress level in the nanowall increases with the extent of lithiation and nearly saturates after  $x_{average}$  exceeds 1.

**Table S1 (a)** Mean stress range and critical radii  $R_c$  in highlighted regions in Figure 5 b, c (at lithiation half cycle with  $x_{average} = 1$ )

Region	A	B	C,F	D,G	E
mean stress range (GPa)	0.25~0.28	0.15~0.25	0.15~0.30	0.30~0.60	0.15~0.18
critical radius $R_c$ (nm)	7.1~8	8~13.3	6.67~13.3	3.33~6.67	11.1~13.3

**Table S1 (b)** mean stress range and critical radii  $R_c$  in highlighted regions in Figure 5d, e (at delithiation half cycle with  $x_{average} = 1$ )

Region	a	b,c,e,g,h,k	d,i	f,j
mean stress range (GPa)	0.35~0.4	0.15~0.35	0.35~1	0.35~0.4
critical radius $R_c$ (nm)	5~5.71	5.71~13.3	2~5.71	5~5.71

### 3. Materials details

The Si thin film is prepared by e-beam deposition under  $4 \times 10^{-7}$  torr. The deposition chamber is pumped down overnight to achieve the a low vacuum level, in order to get high purity Si. EDS data of Si thin film on stainless steel substrate shows a high purity of 96.33wt% of Si with impurities of C, O, Al of 1.38wt%, 1.20wt%, 1.09wt%, respectively. The Al impurity may be a residual impurity from the e-beam evaporator crucible. C and O may come from the substrate and surface oxidation of the thin film.

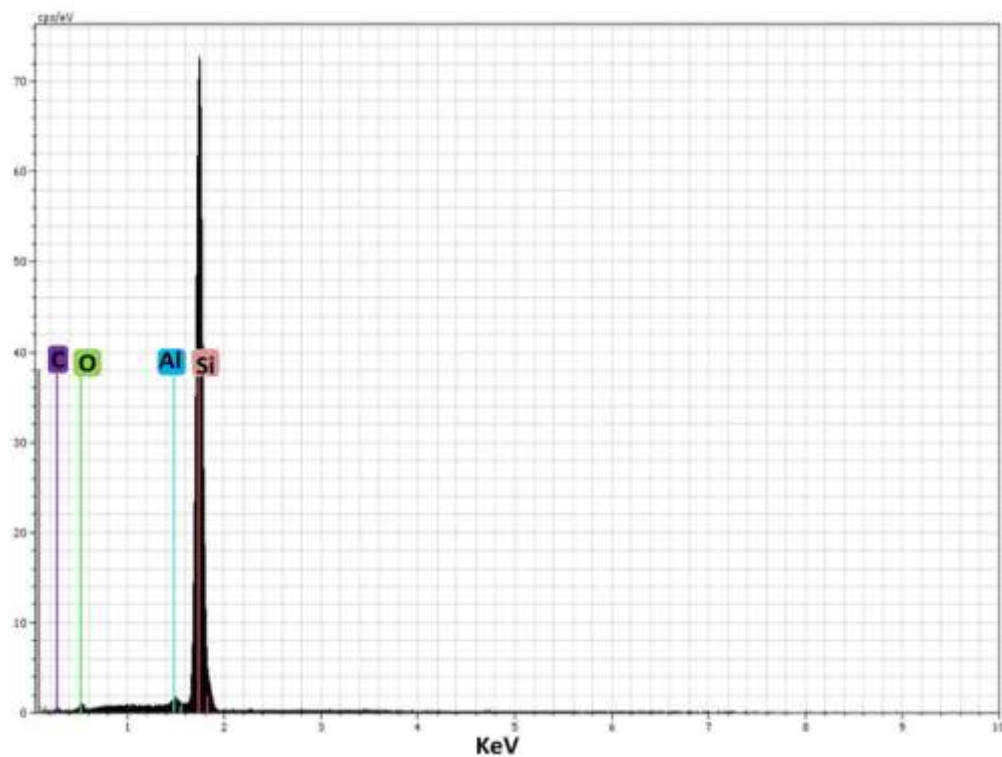


**Figure S5.** EDS results of prepared e-beam deposited a-Si thin film

**Table S2.** Si thin film composition by EDS

El	An	Series	Concentration(wt%)	C atom(at. -%)	Err (%)
C	6	K-series	1.38	3.13	0.4
O	8	K-series	1.20	2.05	0.3
Al	13	K-series	1.09	1.10	0.1
Si	14	K-series	96.33	93.72	4.5

**Figure S6** shows the EDS mapping (top view) of the nanowall structure, all from the same area. From **Figure S6a** and **S6c** we can clearly see the nanoimprint nanowall arrays. However **Figure S6b** shows the whole area is covered by Cr (Cr mask and binding enhancing layer). This proves there are residual Cr mask on top of Si nanowall.

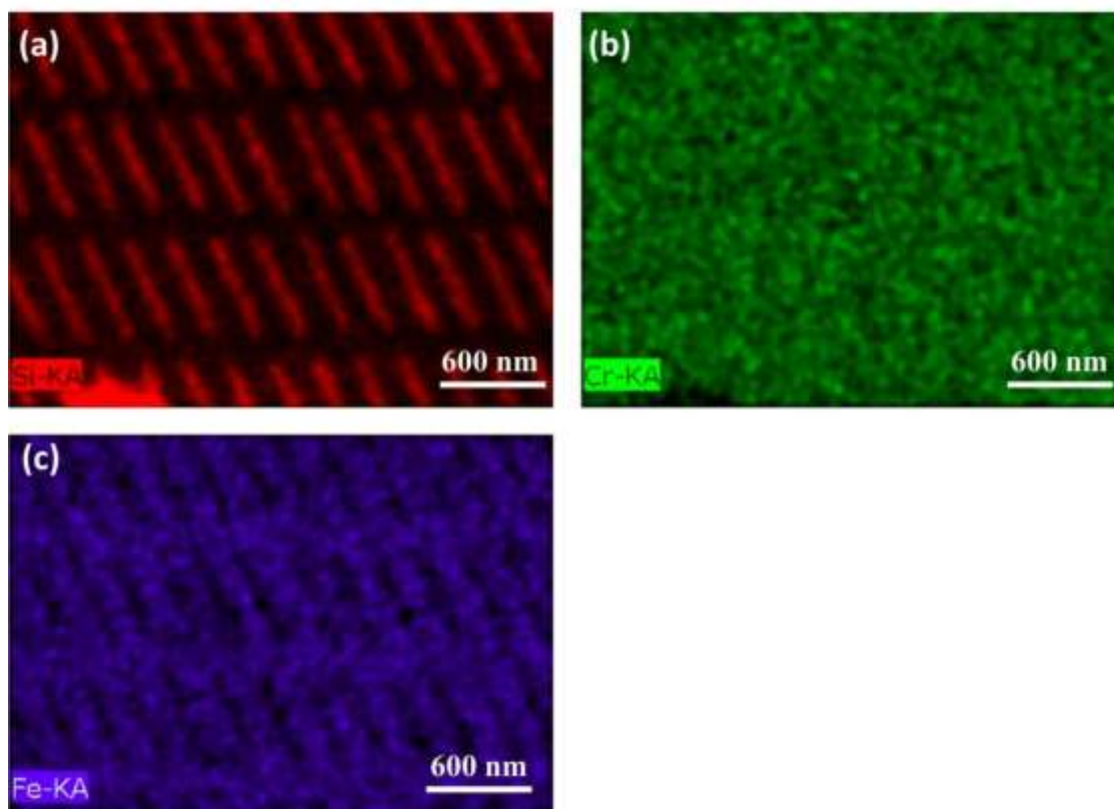


**Figure S6.** EDS mapping result of Si nanowall structure before cycling, in the same area (a) Si mapping; (b). Cr mapping; (c). Fe mapping

## References and Notes

1. Zhao, K.; Pharr, M.; Wan, Q.; Wang, W. L.; Kaxiras, E.; Vlassak, J. J.; Suo, Z., Concurrent Reaction and Plasticity during Initial Lithiation of Crystalline Silicon in Lithium-Ion Batteries. *Journal of The Electrochemical Society* 2012, 159, A238-A243.
2. Obrovac, M. N.; Christensen, L.; Le, D. B.; Dahn, J. R., Alloy Design for Lithium-Ion Battery Anodes. *Journal of The Electrochemical Society* 2007, 154, A849-A855.
3. Haftbaradaran, H.; Gao, H.; Curtin, W. A., A surface locking instability for atomic intercalation into a solid electrode. *Applied Physics Letters* 2010, 96, 091909-3.